DTIC COPY

ON THE ORIGINS OF SOLAR EIT WAVES

E. W. CLIVER
Space Vehicles Directorate, Air Force Research Laboratory, Hanscom AFB, MA 01731

M. LAURENZA AND M. STORINI
Istituto di Fisica dello Spazio Interplanetario, INAF, I-00133 Rome, Italy

AND

B. J. THOMPSON
NASA Goddard Space Flight Center, Greenbelt, MD 20771

20060214 012

ABSTRACT

Approximately half of the large-scale coronal waves identified in images obtained by the Extreme-Ultraviolet Imaging Telescope (EIT) on the *Solar and Heliospheric Observatory* from 1997 March to 1998 June were associated with small solar flares with soft X-ray intensities below C class. The probability of a given flare of this intensity having an associated EIT wave is low. For example, of ~8,000 B-class flares occurring during this 15 month period, only ~1% were linked to EIT waves. These results indicate the need for a special condition that distinguishes flares with EIT waves from the vast majority of flares that lack wave association. Various lines of evidence, including the fact that EIT waves have recently been shown to be highly associated with coronal mass ejections (CMEs), suggest that this special condition is a CME. A CME is not a sufficient condition for a detectable EIT wave, however, because we calculate that ~5 times as many front-side CMEs as EIT waves occurred during this period, after taking the various visibility factors for both phenomena into account. In general, EIT wave association increases with CME speed and width.

Subject headings: Sun: corona — Sun: coronal mass ejections (CMEs) — Sun: flares

1. INTRODUCTION

Using cinematography of high-cadence (six frames per minute) Hα images, Moreton (1960; see also Moreton & Ramsey 1960; Athay & Moreton 1961) discovered large-scale propagating chromospheric disturbances. Four events were observed during 1959 in which "a flare unambiguously resulted in abrupt activation of one or more absorption filaments, situated in preferred directions, at distances of 150,000–700,000 km from the flare." The inferred speed at which the disturbances propagated from the flare site was ~1000 km s^{-1}. Dodson & Hedeman (1968) showed that for some cases, Moreton waves, as they came to be called, could be broken into a leading redshifted component, indicating depression of the solar atmosphere, followed by a blueshifted component, representing subsequent relaxation. Uchida (1968) modeled Moreton waves as the "sweeping skirts" of flare-induced hydromagnetic shock waves that expanded upward into the corona, and he subsequently (Uchida 1973, 1974a, 1974b) linked the waves to metric type II bursts. Smith & Harvey (1971) summarized the findings on Moreton waves a decade following their discovery, and then, with few exceptions (e.g., Harvey et al. 1974), the study of these phenomena went dormant for ~25 years. During this hiatus, the key development bearing on the understanding of large-scale waves in the solar atmosphere was the discovery of coronal mass ejections (CMEs; Koomen et al. 1974, and references therein).

The Extreme-Ultraviolet Imaging Telescope (EIT; Delaboudinière et al. 1995) on the *Solar Heliospheric Observatory* (*SOHO*; Domingo et al. 1995), launched in 1995 December, made it possible to image wave motions in the solar corona (Thompson et al. 1998, 1999, 2000b) at nonradio wavelengths and initiated a resurgence of studies of disturbances propagating in the solar atmosphere. EIT waves are observed as moving fronts of increased emission, with typical speeds of 200–400 km s^{-1} (Klassen et al. 2000). They are generally faint (<20% increase above background), large-scale (a few arcminutes in thickness, with angular spans ranging from a few arcminutes to over a solar radius) features that in some cases travel across the entire disk of the Sun. Recent work (Pohjolainen et al. 2001; Warmuth et al. 2004a, 2004b; Cliver et al. 2004; cf. Zhukov & Auchère 2004) suggests that the synthesis of metric type II bursts and chromospheric Moreton waves proposed by Uchida can be extended to the newly discovered EIT waves.

The question of the origins of EIT waves remains open, however. The debate exactly mirrors that on the origin of metric type II bursts (see the exchange between Cliver [1999] and Gopalswamy et al. [1999]). Do EIT waves originate in flares—explosive heating and expansion of the low corona—or do they result from magnetically driven mass motions, i.e., CMEs?

Biesecker et al. (2002) determined flare and CME associations for a catalog of EIT waves compiled for the period from 1997 March to 1998 June (Thompson & Myers 2005). They concluded that the correlation of EIT waves with flares is significantly weaker than that found between EIT waves and CMEs. In particular, the association of the "highest rated" waves on or near the solar limb (>60° from central meridian) with CMEs approached 100%. In the present study, we compare the numbers of EIT waves, flares, and CMEs during the 15 month period covered by the catalog to gain further insight on the origins of EIT waves. Our analysis is presented in § 2, and the results are discussed in § 3.

2. ANALYSIS

2.1. *Association of EIT Waves with Soft X-Ray Flares*

Thompson & Myers (2005) cataloged 176 EIT waves between 1997 March 24 and 1998 June 24. The start date for the

TABLE 1

QUALITY RATING AND CONFIDENCE LEVELS FOR EIT WAVES (FROM THOMPSON & MYERS 2005)

Quality Rating	Description/Criteria	Confidence Level (%)
Q0	Very low reliability; either a bright front with no clear evidence of propagation, an extremely faint disturbance, or unusual structure. We suspect that this category includes a number of weak waves as well as unrelated phenomena.	<10
Q1	Low reliability; either a faint bright front with structure that may resemble those in the class 5 events, or some evidence of a propagating brightening.	10–25
Q2	Low reliability; faint to strong bright front or a brightening that is moving.	25–50
Q3	Intermediate reliability; either multiple images of a propagating brightening or a clear observation of a bright front that is very similar in structure to the class 5 waves.	50–75
Q4	High reliability; multiple images of a propagating brightening, spatial correspondence from one image to the next.	>75
Q5	Nearly definite reliability; clear evidence of a propagating bright front in multiple images, extent of the wave is far from other activity such that the transient increase in emission is able to be distinguished from other evolving features.	100

compilation marks the onset of regular high-cadence (more than one image every 20 minutes; typically 12–18 minutes between images) EIT observations and the end date corresponds to the onset of the 4 month interruption of *SOHO* observations in mid-1998. The 176 events span a range of confidence levels, ranging from "candidate" events, which were either weak or had insufficient data coverage, to waves that were well defined and easily identified in the data. A "quality rating" (Q), ranging from Q0 (lowest confidence) to Q5 (highest), was assigned to each of the events. The Q levels, described in detail in Table 1, indicate the level of certainty that a transient is a true wave rather than some other kind of disturbance. In addition to the Q rating, the catalog includes information on wave timing, location, and speed.

In Table 2, we give the numbers of EIT waves associated with soft X-ray flares in the A, B, C, M, and X 1–8 Å peak intensity (I) classes (A class [10^{-8} W m$^{-2} \leq I \leq 9.9 \times 10^{-8}$ W m^{-2}]; B class [10^{-7} W m$^{-2} \leq I \leq 9.9 \times 10^{-7}$ W m^{-2}]; C class [10^{-6} W m$^{-2} \leq I \leq 9.9 \times 10^{-6}$ W m^{-2}]; M class [10^{-5} W m$^{-2} \leq I \leq 9.9 \times 10^{-5}$ W m^{-2}]; X class [10^{-4} W m$^{-2} \leq I \leq 9.9 \times 10^{-4}$ W m^{-2}]). When making these associations, we listed the largest flare that could plausibly be associated with the EIT wave, favoring flares that began between the times of the preceding EIT image without a wave and the first image in which the wave was observed (based on the timing information given in the catalog of Thompson & Myers 2005). When no such flare existed, we simply listed the background level (cf. Biesecker et al. 2002). As was done by Biesecker et al. (2002), we eliminated 38 limb events (those having listed source longitudes of ±90°) from further consideration because of possible occultation of the soft X-ray source. In Table 2, we break the associations between high confidence (Q ≥ 3) and low confidence or candidate (Q ≤ 2) events.

These results are completely consistent with those shown in Figure 2 of Biesecker et al. (2002).

In the right-hand column of Table 2 it can be seen that 54% (75/138) of all EIT waves on the visible disk during this period (Q0–Q5) were associated with flares of B-class or smaller. The percentage of EIT waves associated with ≤B-class flares ranged from 60% for lower quality (Q ≤ 2) waves to 41% for high-quality (Q ≥ 3) waves. If we weight the number of events in each soft X-ray class—Q bin by the confidence levels (probability that a wave is a propagating wave front and not another form of transient brightening) from Table 1, we find that 46% (22/48) of the probable events during this period are associated with B-class or smaller flares.

Examples of well-defined EIT waves accompanied by weak flares are shown in Figures 1 and 2. The 1997 October 11 EIT wave (Fig. 1) had a quality rating of Q4 and was associated with a B4.8 soft X-ray flare that arose in NOAA AR 8092, a small and simple active region (McIntosh Classification AXX, 1 spot, 10 millionths of a solar hemisphere [MSH]). Similarly, the event on 1998 March 10 (Q3, B1.3) shown in Figure 2 originated in a spotless area between two modest NOAA sunspot groups (NOAA AR 8174 [BSO, 7 spots, ∼50 MSH] and 8176 [DAO, 15 spots, ∼130 MSH]). Additional examples of well-defined EIT waves with weak (or no) flares have been discussed by Biesecker et al. (2002; 1997 October 23; Q4, <A3) and Cliver et al. (2004; 1998 January 27; Q3, B2 [also Gopalswamy & Thompson 2000]). The EIT waves on 1997 October 11 and 1998 January 27 were associated with metric type II bursts (Solar-Geophysical Data Prompt Reports).

B-class and smaller flares occur frequently on the Sun. In fact, it is not possible to make counts of such flares during periods of high activity when the *GOES* 1–8 Å background can rise to the

TABLE 2

ASSOCIATION OF EIT WAVES WITH Q ≤ 2 AND Q ≥ 3 QUALITY RATINGS WITH *GOES* 1–8 Å FLARES OF DIFFERENT PEAK INTENSITY CLASSES

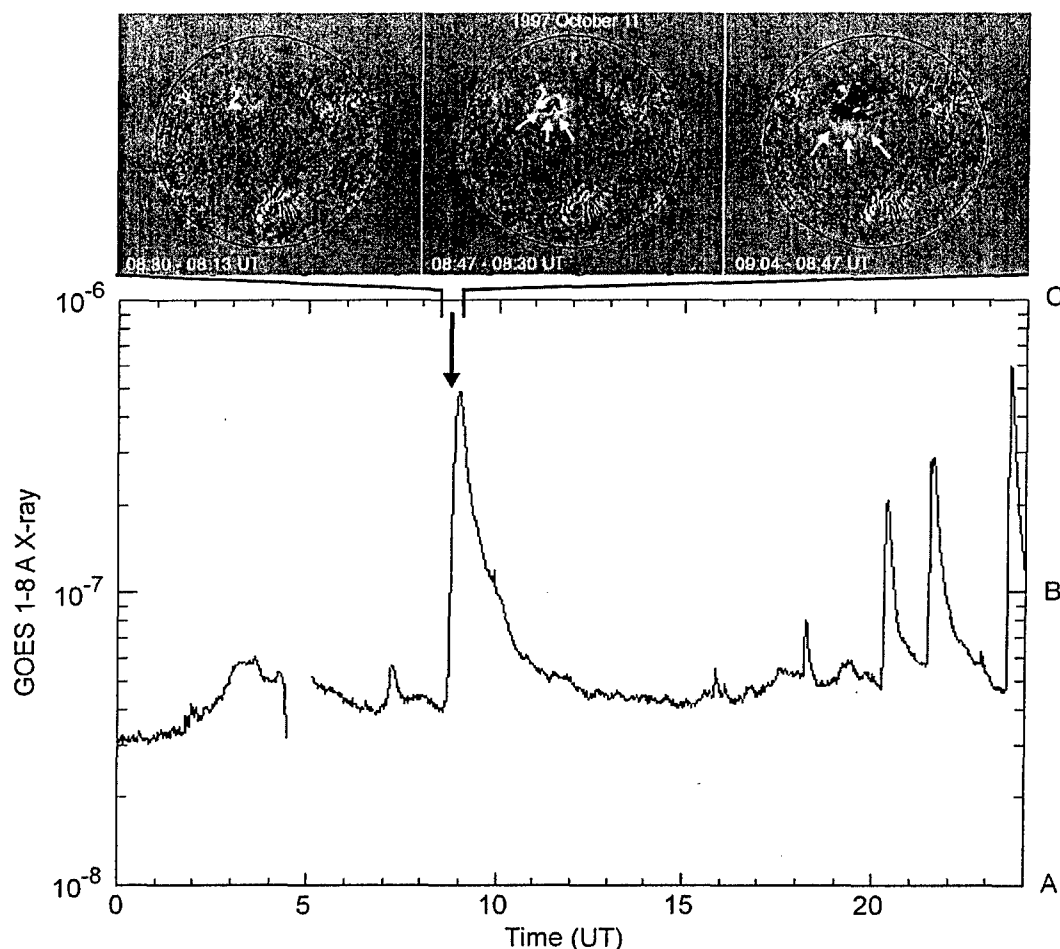| *GOES* 1–8 Å Class	No. (%) of Q ≤ 2 of Waves	No. (%) of Q ≥ 3 of Waves	Total
A	16 (16)	1 (3)	17 (12)
B	44 (44)	14 (38)	58 (42)
C	30 (30)	11 (30)	41 (30)
M	8 (8)	7 (19)	15 (11)
X	3 (3)	4 (11)	7 (5)
Total	101	37	138

Fig. 1.—*Top*: EIT running difference images showing the development of the wave on 1997 October 11. White arrows indicate the leading edge of the wave. *Bottom*: *GOES* 1–8 Å plot for 1997 October 11, with the B4 soft X-ray flare associated with the wave indicated by an arrow. "A," "B," and "C" in the right-hand margin indicate *GOES* peak soft X-ray classes.

C2 level or higher. In order to obtain a count of B-class flares during the period of interest, it is necessary to construct a size distribution for larger flares and extrapolate to lower peak flux values. For the interval from 1997 March 24 to 1998 June 24, the *Boulder Preliminary Report and Forecast of Solar Geophysical Data* lists 698 C-class flares, 58 M-class flares, and 7 X-class events. From these counts, we use a power-law fit[1] to estimate that 7868 (+2243, −1538) B-class flares occurred during the 15 month period considered by Thompson & Myers (2005), ∼15 events per day on average. The probability of a flare of this intensity giving rise to a detectable EIT wave is small. Less than 1% (58/7868) of the B-class flares were linked to EIT waves (of any Q rating). For C-class flares the EIT wave association rate is only ∼6% (41/698).

What distinguishes the small percentages of B-class and C-class soft X-ray flares associated with EIT waves from the great bulk of events of comparable sizes that lack such association? Clearly some special condition is needed. Biesecker et al.

[1] The counts of C-, M-, and X-class flares indicate a power-law slope of roughly −1.0 for the distribution of soft X-ray peak intensities, significantly below the −1.8 value obtained by Drake (1971; see Hudson 1978). A steeper slope would imply an even higher estimate of the number of B-class flares. A correction to the number of C-class bursts to compensate for the fraction of the time (∼5%) that the background soft X-ray flux is above C level during the 15 month interval does not significantly increase the slope of the distribution.

(2002) analyzed the events in the Thompson & Myers (2005) catalog for CME association (taking both wave quality rating and CME observability into account) and found that $Q \geq 2$ EIT waves are highly associated (30/33 cases) with CMEs, based on the temporal/spatial correlation of the two phenomena. Following Biesecker et al. (2002), it is a small step to suggest that the special condition for EIT wave occurrence is a CME.

Before leaving this section, it is necessary to comment on trends in the data between flare size and EIT wave occurrence and quality. The EIT wave association rate increases with flare size, from ∼1% and ∼6%, respectively, for B-class and C-class flares to ∼26% (15/58) for M-class flares, and 100% (7/7) for X-class flares. This trend reflects the relationship found between flare size and the rate of CME association (Andrews 2003; Yashiro et al. 2005). Andrews (2003) found that ∼55% of M-class flares and 100% of X-class flares (from anywhere on the visible disk) had associated CMEs, while Yashiro et al. (2005) obtained CME association rates of ∼20%, ∼50%, and ∼90%, respectively, for front-side C-, M-, and X-class flares. The EIT wave Q rating also increases as one goes from smaller to larger flares (Table 1). Only about ∼6% of the EIT waves associated with A-class flares have $Q \geq 3$ ratings versus 56% of X-class flares. We suspect that this tendency is a manifestation of the Big Flare Syndrome (Kahler 1982), whereby the number of phenomena associated with a flare (or alternatively, the visibility/clarity/intensity of such
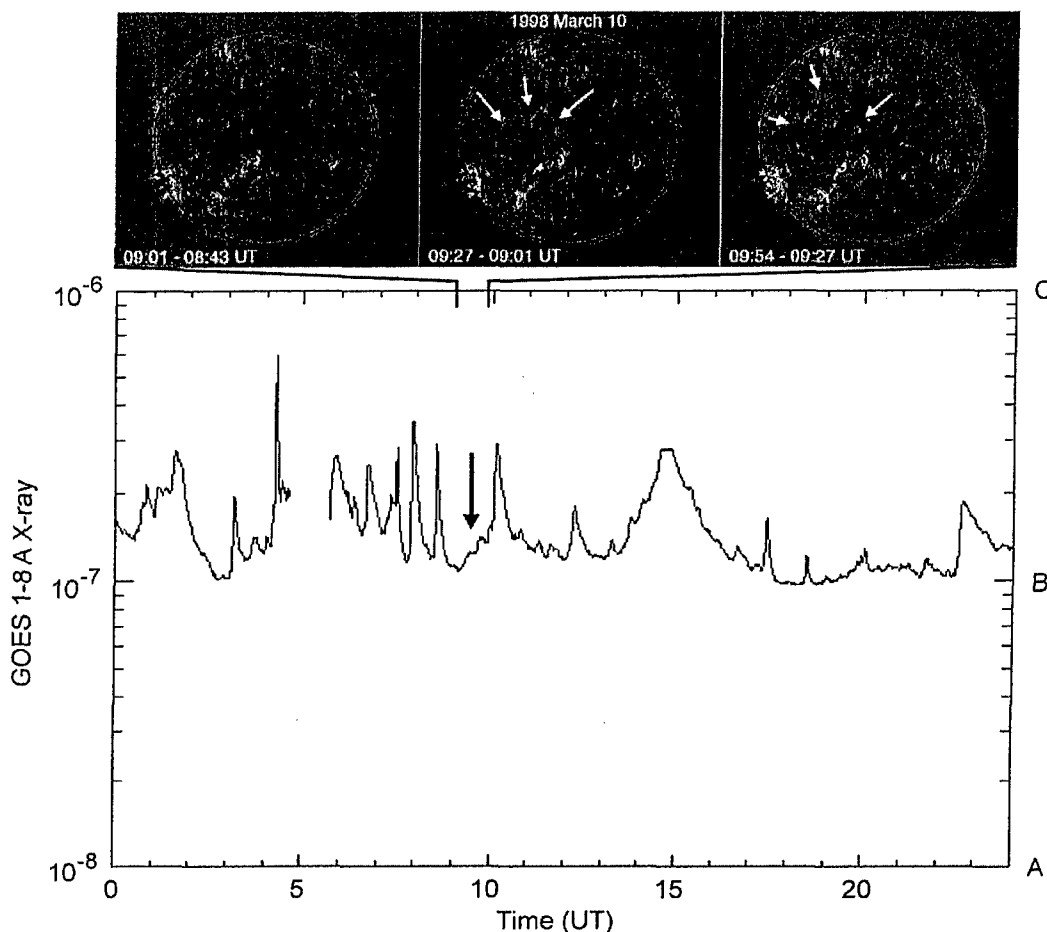
FIG. 2.—*Top*: EIT running difference images showing the development of the wave on 1998 March 10. White arrows are used to indicate the leading edge of the wave. *Bottom*: *GOES* 1–8 Å plot for 1998 March 10, with the B1 soft X-ray flare associated with the wave indicated by an arrow. "A," "B," and "C" in the right-hand margin indicate *GOES* peak soft X-ray classes.

phenomena) can be expected to increase with flare size. Such correlations need not imply a causal relationship between the flare and the associated phenomenon. Despite the observed upward trend in Q rating with flare size, Table 2 shows that C-class and smaller flares accounted for ~85% of all EIT waves during this interval and ~70% of well-defined events, supporting our viewpoint that EIT waves owe their existence to CMEs rather than to their associated flares.

2.2. EIT Waves and CMEs

Biesecker et al. (2002) stated, "If an EIT wave is observed, there must be a CME . . . ." They were careful to note, however, that the converse is not necessarily true. Similarly, we are not saying that all B-class or C-class flares with CMEs will produce EIT waves. The catalog of CMEs[2] observed by the Large Angle Spectrometric Coronagraph (LASCO; Brueckner et al. 1995) on *SOHO* lists a total of 829 CMEs for the period from 1997 March 24 to 1998 June 24, a factor of ~5 more than the 176 EIT waves (of all Q ratings) listed in the Thompson & Myers (2005) catalog.

2.2.1. CME and EIT Wave Visibility

In this section we attempt to compare the number of CMEs originating on the front side of the Sun with the number of EIT

[2] See http://cdaw.gsfc.nasa.gov/CME_list/.

waves occurring on the visible solar disk during the 15 month period of interest. These numbers will differ from those given above (829 and 176, respectively) because of the event observability or "visibility" of both phenomena and the different instrumental duties cycles of LASCO and EIT.

We consider the CMEs first. Coronagraphs are capable, at least to first order, of recording CMEs from the front side and the back side of the Sun equally well, so the total CME count is reduced by a factor of 2, from 829 to 415, to obtain an estimate of the number of front-side events. The LASCO duty cycle from 1997 March to 1998 June was relatively constant at ~95% (dead time is given by the sum of gaps >3 hours in the C2 [2–6 $R_\odot$] coronagraph; N. Gopalswamy 2005, private communication), implying a corrected count of 435 CMEs (415/0.95).

This number must be adjusted further upward, however, because coronagraphs are most sensitive to events in the plane of the sky and CMEs originating near disk center may be missed (Webb & Howard 1994). The visibility function for LASCO gives the fraction of front-side CMEs that the coronagraph observes in various longitude ranges, with the fraction being highest near the limb. The LASCO visibility function can be inferred crudely from the study of Biesecker et al. (2002) if we assume that all of the Q3–Q5 events are true waves. From Table 3 in Biesecker et al. (2002), it can be seen that 100% (11/11) of Q ≥ 3 waves from longitudes >60° have associated CMEs versus

~60% (20/34) of such waves from longitudes <60°. Because CMEs are equally likely to arise at any longitude, we can use these percentages to calculate the number of front-side CMEs that occurred from 1997 March to 1998 June. We assume that during this period LASCO observed 100% of the CMEs originating within 30° of the solar limbs and 59% of those within 60° of central meridian to obtain an occurrence rate of ~600 front-side CMEs.

The increase in the number of CMEs from 435 to 600 implies that LASCO observes ~72% of all CMEs. This is less than the 95% figure reported by St. Cyr et al. (2000) from a preliminary analysis based on metric type II bursts but higher than the percentage that can be inferred from the recent study of Yashiro et al. (2005). Those authors concluded that approximately half of all CMEs associated with C-class soft X-ray flares were not observed by LASCO. From an analysis of *Solar Maximum Mission* (*SMM*) coronagraph data for 1986–1987, Harrison (1995) deduced that 86% of all CMEs were associated with C-class or smaller flares. Ignoring the effects of the differing sensitivities of the *SMM* and *SOHO* coronagraphs, this implies that ~40% of all CMEs are missed by LASCO.

In contrast to CMEs, EIT waves are most easily identified near the center of the disk, where effects of foreshortening are minimized. Of the 176 EIT waves listed by Thompson & Myers (2005), 84 originated within 30° of disk center, versus 33 from middle longitudes (31°–60° east and west) and 59 events from within 30° of either limb. (The 59 events in the limbmost bin includes 38 events with listed longitudes of ±90°; some of these 38 events originated from beyond the limb, inflating the bin count. In addition, the relatively high count in this bin suggests that EIT waves are easier to observe off-limb than on the disk, countering the foreshortening effect.) We assume that the disk center count (84) gives the correct number of waves for a 60° range of longitude and weight these 84 Q0–Q5 events by the probability levels in Table 1 to obtain 30 "definite" waves per 60° bin and a total of 90 front-side waves during this period. Correcting this number for the average ~60% duty cycle of EIT during this period (monthly range ~40%–70%; A. Young 2005, private communication), based on a dead time summation of gaps of >20 minutes between 195 Å images, we obtain 150 front-side EIT waves.

Thus, we deduce that CMEs from front-side solar eruptions occurred 4 times more frequently than EIT waves (600/150) on the visible disk from 1997 March to 1998 June. Recently, Andrews (2002) has argued that CMEs should be more visible from front-side than back-side eruptions. Although he did not specify by how much, it seems unlikely that the imbalance could be more than, say, 1.5 : 1. Such a disparity (which remains to be demonstrated) would increase the number of front-side CMEs to ~500 before applying duty cycle and visibility corrections, and ~725 CMEs after, for a CME/wave ratio of 4.8.

2.2.2. *Effect of CME Speed and Width on EIT Wave Association*

From energy considerations, we would expect EIT waves to be preferentially associated with fast/wide CMEs. In the Thompson & Myers (2005) catalog, 15 Q3–Q5 events have listed source regions within 45° of the solar limb (where the projection effect on CME speeds is reduced). Of these 15 events, 14 had associated CMEs and 13 of these had speeds >400 km s^{-1}. The median speed of the 14 CMEs is ~730 km s^{-1} (range from ~200 to 1600 km s^{-1}). For comparison, the median speed of all limb CMEs is ~400 km s^{-1} (Burkepile et al. 2004).

The fastest (>1000 km s^{-1}) CMEs, originating anywhere on the Sun, during the 15 month interval were accompanied by EIT waves 60% of the time (12 of 20 cases with EIT coverage; waves of any Q rating included). For CMEs with speeds in the range from 800 to 1000 km s^{-1}, the association rate decreased to ~50% (7/15), while for CMEs with speeds from 700 to 800 km s^{-1}, the association rate was ~30% (6/21). These CME-EIT wave association rates compare with the overall uncorrected (raw) association rate of ~20% (176/829). Although there is a definite trend for EIT wave association to decrease with decreasing CME speed, there is no clear dividing line in speed that separates CMEs with EIT waves from those that lack them.

The above association rates were determined without regard to CME location on the Sun. The CME–EIT wave association rate for CMEs originating on the visible disk (including beyond-the-limb CMEs with observable post flare loop systems in EIT) is 80% (12/15) for CMEs with speeds >1000 km s^{-1} and drops to ~40% for CMEs with speeds from 700 to 800 km s^{-1}.

CME width is also an important factor for EIT wave formation/detection. The median width of the 25 fast (≥700 km s^{-1}) CMEs, arising anywhere on the Sun, during this period that were associated with EIT waves (of any Q rating) was 165°. In comparison, the median width of the 31 such CMEs that lacked EIT waves was 61°. If, in order to minimize the propagation effect, we consider only the 18 EIT waves (with fast CMEs) that originated within 30° of the solar limbs, we find that the associated CMEs have a median width of 138°, still more than twice that obtained for all 31 non–wave-associated fast CMEs.

Previously it has been noted that narrow CMEs (widths <60°) are not well associated with either radio type II bursts (Gopalswamy et al. 2001) or solar energetic particles (Kahler & Reames 2003). Fifteen of the 31 fast CMEs without associated EIT waves had angular spans <60° versus 2 of the 25 fast CMEs with EIT waves.

2.2.3. *Effect of Solar Cycle Phase*

There is an additional factor that bears on EIT wave detectability following a CME. Our study was conducted for a period from solar minimum through the midrise of solar cycle 23. By definition, the Sun is relatively free from spots and active regions during these times. Thompson et al. (1999) noted that EIT waves are best observed in "quiet-Sun" regions. The waves propagate through such regions, deflecting away from high–Alfvén speed active regions and disappearing from view when they reach filament channels and coronal holes. At a typical EIT cadence (~15 minutes), a 300 km s^{-1} disturbance can travel ~40% of a solar radius. As a result, it is easier to detect waves in the EIT data near solar minimum conditions, when there are large expanses of quiet-Sun regions.

As mentioned above, only 3 of 15 high-speed (>1000 km s^{-1}) front-side/near-limb CMEs that were observed during the 15 month period we considered lacked EIT waves. We examined each of these three cases; EIT images for the 1998 January 3 eruption are shown in Figure 3. The figure's three frames consist of a 195 Å subfield at 07:23 UT, a 304 Å subfield at 07:29 UT, and the difference between the 09:20 and 08:59 UT 195 Å images. The label "A" indicates the polar coronal hole boundary, "B" marks the erupting filament (and the posteruptive loops in the difference image), and "C" indicates a large active region and filament channel, which was not involved in the eruption but which lies on the disk of the Sun adjacent to the erupting filament. Because EIT waves do not propagate beyond filament channels and coronal holes, and because they are rapidly deflected by active regions, it is clear that it would have been very difficult to observe a wave in this case. Of the two other fast CMEs without waves, one (1998 June 5) was similarly "fenced in," while the other (1998 April 24) lacked obvious local impediments to wave observation.
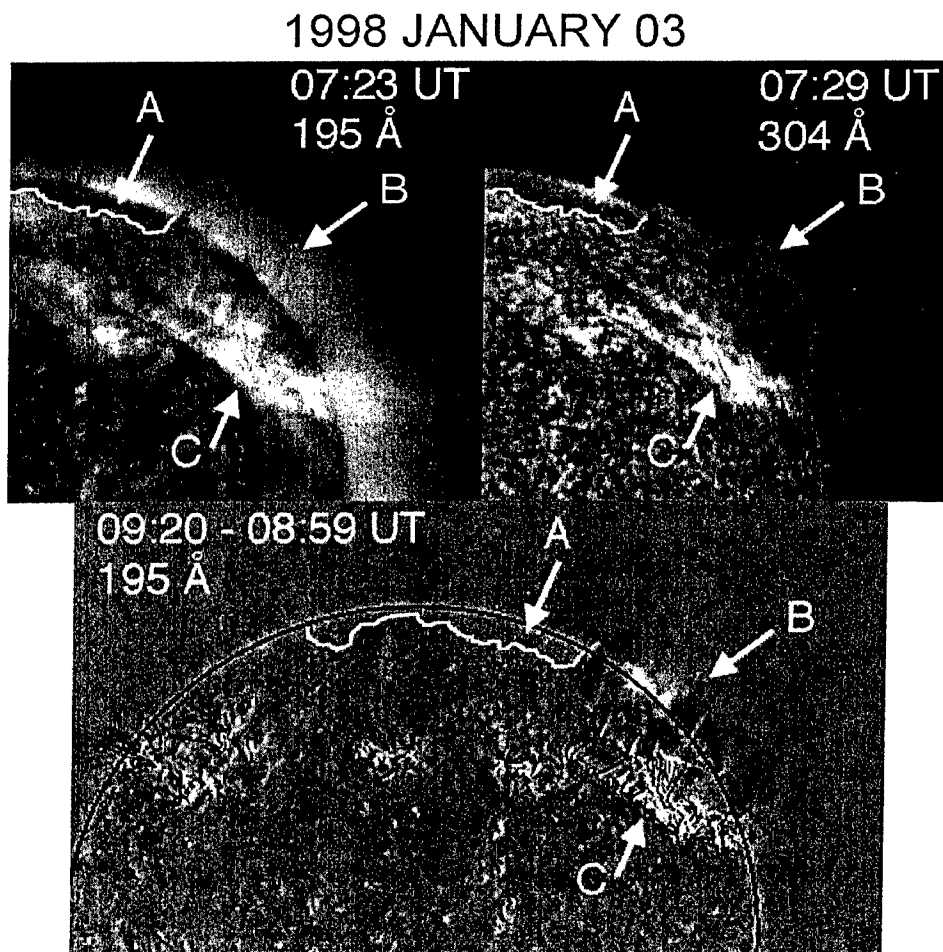
1998 JANUARY 03

Fig. 3.—EIT images of a solar eruption on 1998 January 3. *Top left*: 195 Å image at 07:23 UT. *Top right*: 304 Å image at 07:29 UT. *Bottom*: 195 Å difference image (09:20–08:59 UT). "A" indicates the polar coronal hole boundary, "B" marks the erupting filament (and the posteruptive loops in the difference image), and "C" denotes a large active region and filament channel that was not involved in the eruption but which lies on the disk of the Sun adjacent to the erupting filament.

Because of the correlation between CME rate and sunspot number (Webb & Howard 1994; Gopalswamy 2004), one would expect the frequency of EIT waves to increase as the solar cycle nears maximum. However, on the approach to solar maximum, the extended quiet-Sun regions that facilitate EIT wave observation become increasingly rare. This trend works in the opposite direction of the increasing CME rate. Do we expect more, or fewer, EIT waves at solar maximum? A preliminary examination of post-1998 EIT data indicates a higher rate of EIT waves, but a much larger proportion of waves with low ($Q \leq 2$) quality ratings. High-cadence imagers, such as the *Transition Region and Coronal Explorer* (*TRACE*; Handy et al. 1999), can help to bridge this gap; if there is more than one image per minute, the wave need only be observed over a very small distance. Wills-Davey & Thompson (1999) describe such an event observed on 1998 June 13 with the *TRACE* experiment. EIT captured only one clear image of the wave, while *TRACE* obtained multiple frames, enabling a detailed description of the propagation and evolution of the disturbance.

3. DISCUSSION

Moreton waves were discovered in 1960, while the general recognition of CMEs dates from the early 1970s. In the decade between these two discoveries, large-scale chromospheric waves

became closely linked with solar flares. Observationally, the wave onset was tied to the flare in both time and space. In their 1971 review, however, Smith & Harvey refrained from calling them flare waves directly and, in order "to minimize prejudicing our discussion of the observational effects of the phenomenon," used the more circumspect term "flare-associated" wave.

There is increasing evidence (e.g., Warmuth et al. 2004a, 2004b; cf. Eto et al. 2002) that the recently discovered EIT waves (Thompson et al. 1998, 1999, 2000b) are the coronal counterparts of Moreton waves and that the chromospheric and coronal waves have a common origin. The nature of that origin is controversial, however, with some favoring a flare-initiated blast wave (Khan & Aurass 2002; Hudson et al. 2003; Warmuth et al. 2004b) and others viewing Moreton and EIT waves as CME-driven phenomena (Cliver et al. 2004), or at least as CME-caused phenomena (e.g., Chen et al. 2002). Our finding in this study that ~50% of all EIT waves (and ~40% of $Q \geq 3$ waves) are associated with small (B-class or smaller) soft X-ray flares—that can occur several tens of times per day during periods of high solar activity—does not support the flare-initiated blast wave scenario. Clearly some special condition is needed to distinguish between small flares that are associated with an EIT wave (see, e.g., Figs. 1 and 2) and the vast majority of flares of the same size that are not. Roberts (1959) initially made this argument in

regard to the relationship between flares and metric type II bursts (many flares, few type II bursts; see Cliver et al. 1999). Since Biesecker et al. (2002) found a strong link between EIT waves and CMEs, we argue that the special condition needed for an EIT wave is a CME. CMEs should be natural drivers for large-scale waves in the solar atmosphere.

Paraphrasing B. J. Thompson et al. (2005, in preparation), it is difficult to envision a scenario in which a CME moving suddenly outward through the corona does *not* result in some sort of propagating disturbance. While waves might result from explosive heating of the solar atmosphere following flares (the blast wave scenario), the existence of many examples of well-defined EIT waves associated with small flares (Table 1) suggests that even in the large flares, it is the CME rather than the flare heating that gives rise to the wave. Proof of the existence of even a small subset of flare-generated EIT waves will require the identification of events that unambiguously lack associated CMEs. To the best of our knowledge no such EIT wave has yet been identified.

Zhang et al. (2001) showed that the rapid acceleration phase of CMEs closely corresponds to the fast rise of soft X-rays, i.e., the flare impulsive phase. Their study provides indirect support for our argument for a CME driver for EIT and Moreton waves in the sense that the temporal relationship between flares and waves that has been traditionally used to support a flare origin for Moreton waves now also applies to CMEs (see Cliver et al. 2004). In addition, recent studies (e.g., Dere et al. 1997; Gallagher et al. 2003) indicate that CMEs can originate in volumes with size scales $\sim 10^5$ km, commensurate with the characteristic initial distance of wave observation from the flare site. Finally, B. J. Thompson et al. (2005, in preparation; see also West & Thompson 2003) present evidence for an organic relationship between EIT waves and EUV dimmings, generally taken to be a surface manifestation of a CME (Hudson et al. 1996; Hudson & Webb 1997; Zarro et al. 1999; Thompson et al. 2000a; Howard & Harrison 2004). They find that the formation and early development of the EIT wave is related to the development of the coronal dimming. In particular, for events close to flare onset, the EIT wave gives the appearance of being wrapped around the dimming region, suggestive of a CME-driven wave.

Gilbert & Holzer (2004) recently reported multiple (five) He I 10830 Å waves in association with a solar eruption on 2000 November 25 and concluded that the third wave identified, beginning at $\sim$18:34 UT, originated in a (X-class) solar flare. These authors also attributed the fourth and fifth waves in this event to the flare, but we focus on the third wave here because it is the one that was earlier (Gilbert et al. 2004) found to be cospatial with an EIT wave. The association of this wave with the flare is problematic because inspection of the *GOES* 1–8 Å record shows that the soft X-ray flux at the time of the first observation of the wave remained below the C2 level and had risen only slightly from the preexisting level. It seems more likely that the wave is associated with the CME, although we note that the first significant (factor of 2) increase in the 1–8 Å flux did not occur until 18:36–18:37 UT. More recently, Balasubramaniam et al. (2005) reported multiple propagating disturbances in Hα in association with an eruption

on 2002 December 19. In this case, the propagating disturbances were attributed to the sequential tearing away of a series of nested magnetic loops in association with a CME.

The fact that approximately 5 times as many front-side CMEs as EIT waves were deduced to occur during the period of our study, after taking the various correction factors into account, shows that a CME is not a sufficient condition for a detectable EIT wave. CME speed appears to be an important factor for wave association, but there is considerable overlap in the speed distributions of CMEs with, and without, associated EIT waves that extends to speeds >1000 km s^{-1}. Similarly, while the median angular width of EIT wave-associated CMEs is much larger than that of CMEs that lack such waves (165° vs. 61°), there is overlap between these two groups for spans >50°. Other factors such as the local environment of the eruption (Fig. 3), the CME acceleration rate (e.g., Plunkett et al. 2000), or the initial temperature of the plasma through which the wave travels (Chen et al. 2005) can also affect the CME-EIT wave association rate.

We would expect the detectability of EIT waves to increase significantly with higher cadence observations and the discrepancy between the numbers of CMEs and EIT waves to decrease accordingly. The fact that 79% (46/58) of all (Q0–Q5) EIT waves originating at longitudes >60° had CME association (Table 3 in Biesecker et al. 2002) supports this expectation. In contrast, the confidence levels in Table 1 that we used in our EIT wave rate calculation imply that only 34% (20/58) of the >60° events were true waves.

Recently, detailed analyses of EIT images for two near-limb solar eruptions (Zhukov & Auchère 2004; see also Delannée 2000, Chen et al. 2005, and Balasubramaniam et al. 2005) have indicated that some large-scale wavelike phenomena are not true waves but rather are local brightenings caused by the sequential opening of magnetic field lines during a CME. Zhukov & Auchère (2004) proposed that EIT waves are bimodal with an eruptive mode (field line opening) followed by a wave mode (see also Chen et al. 2005). Alternatively, Thompson et al. (2000b) hypothesized that the relatively sharp aspect of some EIT waves observed close to flare onset corresponds to a piston-driven phase, while diffuse fronts observed far from the flare site (and transient dimming region) later in the event reflect a freely propagating phase. For either of these two scenarios (Zhukov & Auchère 2004; Thompson et al. 2000b), our comparison of the occurrence rates of EIT waves, flares, and CMEs argues that a CME is the essential feature that distinguishes the small minority of flares that exhibit large-scale propagating coronal disturbances from the great bulk that do not.

REFERENCES

Andrews, M. D. 2002, Sol. Phys., 208, 317
———. 2003, Sol. Phys., 218, 261
Athay, R. G., & Moreton, G. E. 1961, ApJ, 133, 935
Balasubramaniam, K. S., et al. 2005, ApJ, 630, 1160
Biesecker, D. A., Myers, D. C., Thompson, B. J., Hammer, D. M., & Vourlidas, A. 2002, ApJ, 569, 1009
Brueckner, G. E., et al. 1995, Sol. Phys., 162, 357

Burkepile, J. T., Hundhausen, A. J., Stanger, A. L., St. Cyr, O. C., & Seiden, J. A. 2004, J. Geophys. Res., 109, 3103
Chen, P. F., Fang, C., & Shibata, K. 2005, ApJ, 622, 1202
Chen, P. F., Wu, S. T., Shibata, K., & Fang, C. 2002, ApJ, 572, L99
Cliver, E. W. 1999, J. Geophys. Res., 104, 4743
Cliver, E. W., Nitta, N. V., Thompson, B. J., & Zhang, J. 2004, Sol. Phys., 225, 105
Cliver, E. W., Webb, D. F., & Howard, R. A. 1999, Sol. Phys., 187, 89

Delaboudinière, J.-P., et al. 1995, Sol. Phys., 162, 291
Delannée, C. 2000, ApJ, 545, 512
Dere, K. P., et al. 1997, Sol. Phys., 175, 601
Dodson, H. W., & Hedeman, E. R. 1968, Sol. Phys., 4, 229
Domingo, V., Fleck, B., & Poland, A. I. 1995, Sol. Phys., 162, 1
Drake, J. F. 1971, Sol. Phys., 16, 152
Eto, S., et al. 2002, PASJ, 54, 481
Gallagher, P. T., Lawrence, G. R., & Dennis, B. R. 2003, ApJ, 588, L53
Gilbert, H. R., & Holzer, T. E. 2004, ApJ, 610, 572
Gilbert, H. R., Holzer, T. E., Thompson, B. J., & Burkepile, J. T. 2004, ApJ, 607, 540
Gopalswamy, N. 2004, in The Sun and the Heliosphere as an Integrated System, ed. G. Poletto & S. Suess (Boston: Kluwer), 201
Gopalswamy, N., & Thompson, B. J. 2000, J. Atmos. Sol.-Terr. Phys., 62, 1457
Gopalswamy, N., Yashiro, Y., Kaiser, M. L., Howard, R. A., & Bougeret, J.-L. 2001, J. Geophys. Res., 106, 29219
Gopalswamy, N., et al. 1999, J. Geophys. Res., 104, 4749
Handy, B. N., et al. 1999, Sol. Phys., 187, 229
Harrison, R. A. 1995, A&A, 304, 585
Harvey, K. L., Martin, S. F., & Riddle, A. C. 1974, Sol. Phys., 36, 151
Howard, T. A., & Harrison, R. A. 2004, Sol. Phys., 219, 315
Hudson, H. S. 1978, Sol. Phys., 57, 237
Hudson, H. S., Acton, L. W., & Freeland, S. L. 1996, ApJ, 470, 629
Hudson, H. S., Khan, J. I., Lemen, J. R., Nitta, N. V., & Uchida, Y. 2003, Sol. Phys., 212, 121
Hudson, H. S., & Webb, D. F. 1997, in Coronal Mass Ejections, ed. N. Crooker, J. Joselyn, & J. Feynman (Washington: AGU), 27
Kahler, S. W. 1982, J. Geophys. Res., 87, 3439
Kahler, S. W., & Reames, D. V. 2003, ApJ, 584, 1063
Khan, J. I., & Aurass, H. 2002, A&A, 383, 1018
Klassen, A., Aurass, H., Mann, G., & Thompson, B. J. 2000, A&AS, 141, 357
Koomen, M. J., Howard, R., Hansen, R., & Hansen, S. 1974, Sol. Phys., 34, 447
Moreton, G. E. 1960, AJ, 65, 494

Moreton, G. E., & Ramsey, H. E. 1960, PASP, 72, 357
Plunkett, S. P., et al. 2000, Sol. Phys., 194, 371
Pohjolainen, S., et al.. 2001, ApJ, 556, 421
Roberts, J. A. 1959, Australian J. Phys., 12, 327
Smith, S. F., & Harvey, K. L. 1971, in Physics of the Solar Corona, ed. C. J. Macris (Dordrecht: Reidel), 156
St. Cyr, O. C., et al. 2000, J. Geophys. Res., 105, 18169
Thompson, B. J., Cliver, E. W., Nitta, N., Delannée, C., & Delaboudinière, J.-P. 2000a, Geophys. Res. Lett., 27, 1431
Thompson, B. J., & Myers, D. C. 2005, ApJS, in press
Thompson, B. J., Plunkett, S. P., Gurman, J. B., Newmark, J. S., St. Cyr, O. C., & Michels, D. J. 1998, Geophys. Res. Lett., 25, 2465
Thompson, B. J., et al. 1999, ApJ, 517, L151
———. 2000b, Sol. Phys., 193, 161
Uchida, Y. 1968, Sol. Phys., 4, 30
———. 1973, in NASA Symp. On High Energy Phenomena on the Sun, ed. R. Ramaty & R. G. Stone (Greenbelt: NASA), 577
———. 1974a, in IAU Symp. 57, Coronal Disturbances, ed. G. Newkirk (Dordrecht: Reidel), 383
———. 1974b, Sol. Phys., 39, 431
Warmuth, A., Vrsnak, B., Magdalenic, J., Hanslmeier, A., & Otruba, W. 2004a, A&A, 418, 1101
———. 2004b, A&A, 418, 1117
Webb, D. F., & Howard, R. A. 1994, J. Geophys. Res., 99, 4201
West, M., & Thompson, B. J. 2003, Eos, Trans. AGU 84(46), Fall Meet. Suppl., Abstract SH22B-01
Wills-Davey, M. J., & Thompson, B. J. 1999, Sol. Phys., 190, 467
Yashiro, S., Gopalswamy, N., Akiyama, S., Michalek, G., & Howard, R. A. 2005, J. Geophys. Res., in press
Zarro, D. M., Sterling, A. C., Thompson, B. J., Hudson, H. S., & Nitta, N. V. 1999, ApJ, 520, L139
Zhang, J., Dere, K. P., Howard, R. A., Kundu, M. R., & White, S. M. 2001, ApJ, 559, 452
Zhukov, A. N., & Auchère, F. 2004, A&A, 427, 705

REPORT DOCUMENTATION PAGE

Public reporting burden for this collection of information is estimated to average 1 hour per response, including the time for reviewing instructions, searching existing data sources, gathering and maintaining the data needed, and completing and reviewing this collection of information. Send comments regarding this burden estimate or any other aspect of this collection of information, including suggestions for reducing this burden to Department of Defense, Washington Headquarters Services, Directorate for Information Operations and Reports (0704-0188), 1215 Jefferson Davis Highway, Suite 1204, Arlington, VA 22202-4302. Respondents should be aware that notwithstanding any other provision of law, no person shall be subject to any penalty for failing to comply with a collection of information if it does not display a currently valid OMB control number. **PLEASE DO NOT RETURN YOUR FORM TO THE ABOVE ADDRESS.**

1. REPORT DATE (DD-MM-YYYY) 17-01-2006	2. REPRINT		3.

4. TITLE AND SUBTITLE
On the Origins of Solar EIT Waves

5a. CONTRACT NUMBER

5b. GRANT NUMBER

5c. PROGRAM ELEMENT NUMBER
61102F

6. AUTHOR(S)
Cliver, E.W., M. Laurenza*, M. Storini*, and B.J. Thompson**

5d. PROJECT NUMBER
2311

5e. TASK NUMBER
RD

5f. WORK UNIT NUMBER
A1

7. PERFORMING ORGANIZATION NAME(S) AND ADDRESS(ES)
Air Force Research Laboratory/VSBXS
29 Randolph Road
Hanscom AFB MA 01731-3010

8. PERFORMING ORGANIZATION REPORT NUMBER

AFRL-VS-HA-TR-2006-1010

9. SPONSORING / MONITORING AGENCY NAME(S) AND ADDRESS(ES)

10. SPONSOR/MONITOR'S ACRONYM(S)
AFRL/VSBXS

11. SPONSOR/MONITOR'S REPORT NUMBER(S)

12. DISTRIBUTION / AVAILABILITY STATEMENT
Approved for Public Release; Distribution Unlimited.

*Instituto di Fisica dello Spazio Interplanetario, Rome Italy, **NASA Goddard Space Flt Ctr, Greenbelt, MD

14. ABSTRACT

Approximately half of the large-scale coronal waves identified in images obtained by the Extreme-Ultraviolet Imaging Telescope (EIT) on the *Solar and Heliospheric Observatory* from 1997 March to 1998 June were associated with small solar flares with soft X-ray intensities below C class. The probability of a given flare of this intensity having an associated EIT wave is low. For example, of ~8,000 B-class flares occurring during this 15 month period, only ~1% were linked to EIT waves. These results indicate the need for a special condition that distinguishes flares with EIT waves from the vast majority of flares that lack wave association. Various lines of evidence, including the fact that EIT waves have recently been shown to be highly associated with coronal mass ejections (CMEs), suggest that this special condition is a CME. A CME is not a sufficient condition for a detectable EIT wave, however, because we calculate that ~5 times as many front-side CMEs as EIT waves occurred during this period, after taking the various visibility factors for both phenomena into account. In general, EIT wave association increases with CME speed and width.

15. SUBJECT TERMS
Sun   Corona   Corona mass ejections   Flares

16. SECURITY CLASSIFICATION OF:

a. REPORT UNCLAS	b.	c. THIS PAGE UNCLAS	17. LIMITATION OF ABSTRACT SAR	18. NUMBER OF PAGES 10	19a. NAME OF RESPONSIBLE PERSON S. W. Kahler

b. ABSTRACT UNCLAS

19b. TELEPHONE NUMBER (include area code)
781-377-9665